Quantum theory of multiwave mixing. X. Two-photon three-level model

Sunghyuck An and Murray Sargent III
Optical Sciences Center, University of Arizona, Tucson, Arizona 85721
(Received 26 September 1988)

We present a fully quantum-mechanical theory of nondegenerate multiwave mixing processes in three-level cascades with a two-photon pump. The explicit formulas for the resonance fluorescence spectrum and the quantum combination-tone source term are derived. The theory is applied to the generation of squeezed states of light. We find almost perfect squeezing for some strong-pump intensities and tunings within the Rabi sidebands. We find good broadband squeezing for low-pump intensities and tunings outside a small region around central tuning. Both cases avoid regions of significant spontaneous emission.

I. INTRODUCTION

Squeezed states of light are those for which the quantum fluctuations in one quadrature phase of the electric field are reduced below the average minimum variance permitted by the uncertainty principle. Such states have potential applications in optical communication systems and gravity-wave detection. Due to the dependence of squeezing on the phase of the electric field, squeezed states have been predicted to occur in phase-sensitive nonlinear optical processes, such as parametric amplification, second-harmonic generation, and four-wave mixing. The first successful generation of squeezed states has been reported by Slusher *et al.*[1] using nondegenerate four-wave mixing. Recently other groups[2–4] have also succeeded in producing squeezed states using different types of nonlinear media.

Previously Sargent, Holm, and Zubairy[5] have derived a theory describing quantum multiwave interactions in a nonlinear one-photon two-level medium, in which the levels are connected by an electric dipole. Later they have applied this theory to analyze the generation of squeezed states and compared to the experimental results of Slusher *et al.* finding reasonably good agreement.[6] The first nondegenerate semiclassical theory of multiwave mixing in a two-photon two-level medium has been given by Sargent *et al.*[7] The quantum theory of multiwave mixing in such a medium has been derived in detail by Holm and Sargent.[8] Recently Capron, Holm, and Sargent have applied the quantum theory of multiwave mixing for the two-photon two-level model to the generation of squeezed states of light.[9]

In this paper we extend the quantum theory of multiwave mixing by Holm and Sargent to treat squeezing in a three-level cascade model with a classical two-photon pump at frequency ν_2 and a cascade of two one-photon transitions at frequencies ν_1 and ν_3 (see Fig. 1). The preliminary result was presented in Ref. 10. The model differs from those studied by Savage and Walls[11] for which all field frequencies are identical.

The experimental observation of the suppression of amplified spontaneous emission by the four-wave-mixing process in this model has been reported by Malcuit, Gauthier, and Boyd.[12] This experiment has been interpreted using classical fields up to fourth order in all mode interactions,[13] while we treat a classical pump to all orders and quantized squeezed modes to first order. Reference 12 also makes the one-photon rotating-wave approximation for the two-photon pump and neglects the population in the intermediate level, while we include the terms dropped in these approximations. Agarwal[14] studied this model using a weak classical two-photon pump and weak quantized side-mode fields. He showed the generation of squeezed states, but simplified his treatment along the lines of Ref. 12 by neglecting dynamic Stark shifts and the population in the intermediate level. In contrast, our treatment allows for more general tuning conditions and nonzero intermediate level population as created by the potentially strong pump field in conjunction with level decays.

The two-photon three-level model is shown in Fig. 1. The upper level a and ground level c have the same parity, but the intermediate level b has an opposite one. Therefore the transitions $a \leftrightarrow b$ and $b \leftrightarrow c$ are dipole al-

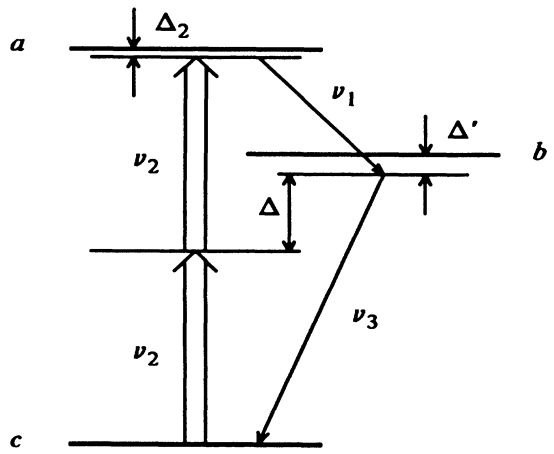

FIG. 1. Three-level cascade model with a two-photon pump.

lowed with frequencies ν_1 and ν_3, respectively, whereas the transition $c \leftrightarrow a$ requires two pump photons with the frequency ν_2. We assume that the one-photon pump detuning $\omega_{bc}-\nu_2$ is sufficiently large that the dipole transition $c \leftrightarrow b$ with pump frequency ν_2 is negligible. The pump frequency ν_2 is approximately one-half the atomic resonance frequency $\omega_{ac} \equiv \omega_a - \omega_c$. The side-mode frequencies ν_1 and ν_3 are assumed to satisfy the conservation condition $\nu_1+\nu_3=2\nu_2$, which gives the relation between the side-mode detuning Δ' and the beat frequency $\Delta \equiv \nu_2-\nu_1$ as $\Delta'=(\omega_{bc}-\nu_2)-\Delta$. We assume that the upper level a decays at the rate Γ_a $(=\Gamma_1+\Gamma_2)$ to the lower levels b and c. Here Γ_1 and Γ_3 are the decay constants for the $a \rightarrow b$ and $b \rightarrow c$ transitions, and Γ_2 allows for nonradiative decay of level a to level c.

Section II summarizes the basic theory of semiclassical single-mode interaction. In Sec. III we use the results of Sec. II to develop the theory of quantum side-mode interactions. Section IV applies the theory to the generation of squeezed states of light.

II. SEMICLASSICAL SINGLE-MODE INTERACTION

In this section we consider the single-mode case and derive the steady-state semiclassical population matrix elements with the population difference decay time T_1. In an interaction picture rotating at the two-photon frequency $2\nu_2$, the equation of motion for the population matrix elements are given by

$$\dot{\rho}_{aa} = -(\Gamma_2+\Gamma_1)\rho_{aa} - (i\mathcal{V}_2\rho_{ca} + \text{c.c.}) , \tag{1}$$

$$\dot{\rho}_{cc} = \Gamma_2\rho_{aa} + \Gamma_3\rho_{bb} + (i\mathcal{V}_2\rho_{ca} + \text{c.c.}) , \tag{2}$$

$$\dot{\rho}_{bb} = \Gamma_1\rho_{aa} - \Gamma_3\rho_{bb} , \tag{3}$$

$$\dot{\rho}_{ac} = -[\gamma_2 + i(\omega_{ac} + \omega_s I_2 - 2\nu_2)]\rho_{ac} + i\mathcal{V}_2(\rho_{aa}-\rho_{cc}) . \tag{4}$$

where $\gamma_2 \equiv 1/T_2$ is the two-photon coherent decay rate between levels a and c, $\mathcal{V}_2 \equiv -k_{ac}\mathcal{E}_2^2/2$ is the effective two-photon interaction energy with the two-photon coefficient k_{ac} defined in Refs. 7 and 8, ω_s is the Stark shift parameter,[7,8] and the two-photon dimensionless intensity I_2 is defined by

$$I_2 = 2|\mathcal{V}_2|\sqrt{T_1 T_2} . \tag{5}$$

Using Eqs. (1) and (2) with the steady-state solution of Eq. (3)

$$\rho_{cc} = (\Gamma_1/\Gamma_3)\rho_{aa} , \tag{6}$$

we find the equation of motion for the population difference $D = \rho_{aa} - \rho_{cc}$

$$\dot{D} = -2\Gamma_a\rho_{aa} - 2(i\mathcal{V}_2\rho_{ca} + \text{c.c.}) , \tag{7}$$

where $\Gamma_a = \Gamma_2 + \Gamma_1$. Combining Eq. (6) and the trace condition

$$\rho_{aa} + \rho_{bb} + \rho_{cc} = 1 , \tag{8}$$

we have

$$\rho_{aa} = \frac{\Gamma_3}{\Gamma_1+2\Gamma_3}(D+1) . \tag{9}$$

Substituting Eq. (9) into (7), we have

$$\dot{D} = -(D+1)/T_1 - 2(i\mathcal{V}_2\rho_{ca} + \text{c.c.}) , \tag{10}$$

where the population difference decay time T_1 is given by

$$T_1 = \frac{1}{\Gamma_a}\left[1 + \frac{\Gamma_1}{2\Gamma_3}\right] . \tag{11}$$

The steady-state solution to the dipole equation (4) is

$$\rho_{ac} = i\mathcal{V}_2\mathcal{D}_2(\Delta_2)D , \tag{12}$$

where $\Delta_2 \equiv \omega_{ac} + \omega_s I_2 - 2\nu_2$ is the pump field detuning as shown in Fig. 1 and the complex Lorentzian denominator

$$\mathcal{D}_2(\Delta_2) = \frac{1}{\gamma_2 + i\Delta_2} . \tag{13}$$

Substituting Eq. (12) into (10), we have

$$\dot{D} = -(D+1)/T_1 - 2RD , \tag{14}$$

where the rate constant

$$R = I_2^2\mathcal{L}_2(\Delta_2)/2T_1 . \tag{15}$$

and the dimensionless Lorentzian

$$\mathcal{L}_2(\Delta_2) = \frac{\gamma_2^2}{\gamma_2^2+\Delta_2^2} . \tag{16}$$

Solving Eq. (14) in a steady state, we find

$$D = \rho_{aa} - \rho_{cc} = \frac{-1}{1+I_2^2\mathcal{L}_2} . \tag{17}$$

Finally, using Eqs. (6), (8), and (17), we have

$$\rho_{kk} = \frac{f_k}{1+I_2^2\mathcal{L}_2} . \tag{18}$$

where $k = a,b,c$, and the probability factors f_k's are given by

$$f_a = \frac{\Gamma_3}{\Gamma_1+2\Gamma_3} I_2^2\mathcal{L}_2 . \tag{19}$$

$$f_b = \frac{\Gamma_1}{\Gamma_1+2\Gamma_3} I_2^2\mathcal{L}_2 , \tag{20}$$

$$f_c = 1 + f_a . \tag{21}$$

The assumptions and method used to obtain Eqs. (18)–(21) are again employed in Sec. III when the quantum-mechanical model is introduced, and we frequently refer to these results.

III. QUANTUM SIDE-MODE INTERACTIONS

The total Hamiltonian $\mathcal{H}$ consists of three parts, the atom, the field, and the interaction:

$$\mathcal{H} = \mathcal{H}_{\text{atom}} + \mathcal{H}_{\text{field}} + \mathcal{H}_{\text{int}} . \tag{22}$$

The atom Hamiltonian is given by

$$\mathcal{H}_{\text{atom}}=\begin{bmatrix}\omega_a & 0 & 0\\ 0 & \omega_b & 0\\ 0 & 0 & \omega_c\end{bmatrix} . \tag{23}$$

The field Hamiltonian is

$$\mathcal{H}_{\text{field}}=\sum_{j=1}^{3}\nu_j a_j^\dagger a_j , \tag{24}$$

and the interaction Hamiltonian is

$$\mathcal{H}_{\text{int}}=\sum_j g_j a_j U_j \sigma_j^\dagger , \tag{25}$$

where a_1 and a_3 are the annihilation operators for the field modes 1 and 3, a_2 is the effective two-photon annihilation operator for the field mode 2, $U_j=U_j(\mathbf{r})$ is the spatial mode factor for the jth field mode, g_j is the atom-field (jth) coupling constant, and the matrices $\sigma_1^\dagger$, $\sigma_2^\dagger$, and $\sigma_3^\dagger$ are defined by

$$\sigma_1^\dagger=\begin{bmatrix}0&1&0\\0&0&0\\0&0&0\end{bmatrix},\quad \sigma_2^\dagger=\begin{bmatrix}0&0&1\\0&0&0\\0&0&0\end{bmatrix},$$
$$\sigma_3^\dagger=\begin{bmatrix}0&0&0\\0&0&1\\0&0&0\end{bmatrix} . \tag{26}$$

We take mode 2 (two-photon pump field) to be classical, undepleted, and arbitrarily intense. Modes 1 and 3 are side-mode quantum fields treated only to second order in amplitude and cannot by themselves saturate the atomic response. The three-level atom interacting with one strong and two weak-field modes involves at least five atom-field levels as shown in Fig. 2. We define an atom-field density operator ρ_{AF} and calculate the reduced electric field density operator ρ that describes the time dependence of the two quantized fields by taking the trace of ρ_{AF} over the atomic states. The states depicted in Fig. 2 have been numerically labeled for notational simplicity. For example, ρ_{53} is equal to

$$\langle a n_1 n_2 n_3|\rho_{AF}|b n_1+1 n_2 n_3\rangle .$$

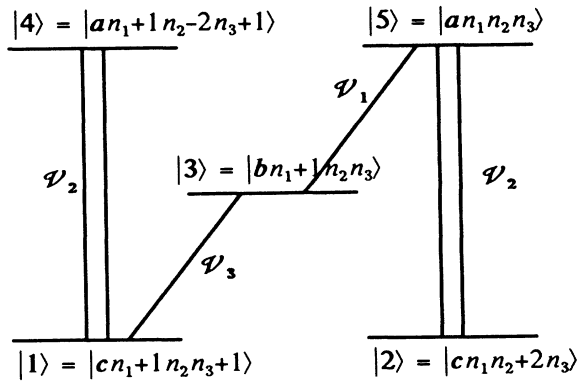

FIG. 2. Five-level atom-field energy-level diagram.

The probability of finding n_1 and n_3 photons in mode 1 and 3 is given by the trace

$$p_{n_1,n_3}=\langle n_1 n_3|\rho|n_1 n_3\rangle$$
$$=\rho_{55}+\rho_{33}|_{n_1\to n_1-1}+\rho_{11}|_{n_{1,3}\to n_{1,3}-1} . \tag{27}$$

The photon rate equation for mode 1 and 3 is given by the corresponding time derivative. To find $\dot\rho_{55}$, $\dot\rho_{33}$, and $\dot\rho_{11}$ and the density-matrix elements coupling to them, we use the basic equation

$$\dot\rho_{AF}=-i(\mathcal{H},\rho_{AF})+r , \tag{28}$$

(where r are relaxation terms) with the Hamiltonian given by Eq. (22). We have

$$\dot\rho_{55}=-(\Gamma_2+\Gamma_1)\rho_{55}-(i\mathcal{V}_2\rho_{25}+i\mathcal{V}_1\rho_{35}+\text{c.c.}) , \tag{29}$$

$$\dot\rho_{33}=\Gamma_1\rho_{55}|_{n_1\to n_1+1}-\Gamma_3\rho_{33}-(i\mathcal{V}_1^*\rho_{53}+i\mathcal{V}_3\rho_{13}+\text{c.c.}) , \tag{30}$$

$$\dot\rho_{11}=\Gamma_2\rho_{44}+\Gamma_3\rho_{33}|_{n_3\to n_3+1}-(i\mathcal{V}_3^*\rho_{31}+i\mathcal{V}_2^*\rho_{41}+\text{c.c.}) , \tag{31}$$

where the one-photon interaction energies $\mathcal{V}_1$ and $\mathcal{V}_3$ are given by

$$\mathcal{V}_1=g_1U_1\sqrt{n_1+1},\quad \mathcal{V}_3=g_3U_3\sqrt{n_3+1} , \tag{32}$$

and the effective two-photon interaction energy $\mathcal{V}_2$ is

$$\mathcal{V}_2=g_2U_2\sqrt{n_2}\cong -k_{ac}\mathcal{E}_2^2/2 , \tag{33}$$

where we neglect the difference between n_2 and n_2+1, i.e., we treat the strong mode classically.

Taking the time derivative of Eq. (27) and substituting Eqs. (29)–(31), we find the photon number equation of motion for the side-mode fields:

$$\dot p_{n_1,n_3}=i\mathcal{V}_1^*\rho_{53}-i(\mathcal{V}_1^*\rho_{53})|_{n_1\to n_1-1}+i(\mathcal{V}_3^*\rho_{31})|_{n_1\to n_1-1}$$
$$-i(\mathcal{V}_3^*\rho_{31})|_{n_{1,3}\to n_{1,3}-1}+\text{c.c.} \tag{34}$$

This equation shows that all we need to find is the dipole elements ρ_{53} and ρ_{31}. Using Eq. (28), we find the equation of motion for ρ_{53},ρ_{31}, and the density-matrix elements coupling to them:

$$\dot\rho_{53}=-[\gamma_1+i(\omega_{ab}-\nu_1)]\rho_{53}$$
$$-i(\mathcal{V}_2\rho_{23}+\mathcal{V}_1\rho_{33}-\mathcal{V}_1\rho_{55})+i\mathcal{V}_3^*\rho_{51} , \tag{35}$$

$$\dot\rho_{31}=-[\gamma_3+i(\omega_{bc}-\nu_3)]\rho_{53}$$
$$-i(\mathcal{V}_3\rho_{11}-\mathcal{V}_3\rho_{33}-\mathcal{V}_2\rho_{34})-i\mathcal{V}_1^*\rho_{51} , \tag{36}$$

$$\dot\rho_{43}=-[\gamma_1+i(\omega_{ab}-\nu_1)]\rho_{43}$$
$$-i(\mathcal{V}_2\rho_{13}-\mathcal{V}_3^*\rho_{41})+i\mathcal{V}_1\rho_{45} , \tag{37}$$

$$\dot\rho_{32}=-[\gamma_3+i(\omega_{bc}-\nu_1)]\rho_{32}$$
$$-i(\mathcal{V}_1^*\rho_{52}-\mathcal{V}_2\rho_{35})-i\mathcal{V}_3\rho_{12} , \tag{38}$$

where we used the conservation condition $\nu_1+\nu_3=2\nu_2$ in Eqs. (36) and (38). To solve Eqs. (35)–(38), we note that

the weak side-mode fields assumption means that $\mathcal{V}_1$ can only appear to second order. This means that the density-matrix elements ρ_{55}, ρ_{33}, ρ_{11}, ρ_{52}, and ρ_{41}, which are multiplied by the weak side-mode interaction potentials, can be factored into the corresponding semiclassical value determined by the $\mathcal{V}_2$ interaction alone, multiplied by the corresponding photon number probability

$$\rho_{55}=\rho_{aa}\rho_{0000} , \tag{39}$$

$$\rho_{33}=\rho_{bb}\rho_{1010} , \tag{40}$$

$$\rho_{11}=\rho_{cc}\rho_{1111} , \tag{41}$$

$$\rho_{52}=i\mathcal{V}_2\mathcal{D}_2(\rho_{aa}-\rho_{cc})\rho_{0000} , \tag{42}$$

$$\rho_{41}=i\mathcal{V}_2\mathcal{D}_2(\rho_{aa}-\rho_{cc})\rho_{1111} , \tag{43}$$

where ρ_{aa}, ρ_{bb}, and ρ_{cc} are given by Eq. (18) and the photon number probabilities ρ_{0000}, ρ_{1010}, and ρ_{1111} are defined as

$$\rho_{0000}=\langle n_1 n_3|\rho|n_1 n_3\rangle=p_{n_1,n_3} , \tag{44}$$

$$\rho_{1010}=\langle n_1+1 n_3|\rho|n_1+1 n_3\rangle , \tag{45}$$

$$\rho_{1111}=\langle n_1+1 n_3+1|\rho|n_1+1 n_3+1\rangle . \tag{46}$$

Similarly, the density-matrix elements ρ_{54}, ρ_{21}, and ρ_{51}, which are also multiplied by the weak side-mode interaction potentials in Eqs. (35) through (38), are given by

$$\rho_{54}=\rho_{aa}\rho_{0011} , \tag{47}$$

$$\rho_{21}=\rho_{cc}\rho_{0011} , \tag{48}$$

$$\rho_{51}=i\mathcal{V}_2\mathcal{D}_2(\rho_{aa}-\rho_{cc})\rho_{0011} , \tag{49}$$

where ρ_{0011} is defined by

$$\rho_{0011}=\langle n_1 n_3|\rho|n_1+1 n_3+1\rangle . \tag{50}$$

To find the density-matrix element ρ_{53} and ρ_{31}, we solve Eqs. (35)–(38) in a steady state. Combining Eqs. (35) and Eq. (38) and solving for ρ_{53} in a steady state, we have

$$\rho_{53}=\frac{-i\mathcal{D}_1[\mathcal{V}_1(-f_a-\mathcal{D}_3^*\mathcal{D}_2^*|\mathcal{V}_2|^2)\rho_{0000}+\mathcal{V}_1 f_b\rho_{1010}+i\mathcal{V}_3^*\mathcal{V}_2(f_c\mathcal{D}_3^*+\mathcal{D}_2)\rho_{0011}]}{(1+\mathcal{D}_1\mathcal{D}_3^*|\mathcal{V}_2|^2)(1+I_2^2\mathcal{L}_2)} , \tag{51}$$

where we used Eqs. (39)–(43) and Eqs. (47)–(49). The complex Lorentzians for mode 1 and 3 are defined by

$$\mathcal{D}_k=\frac{1}{\gamma_k+i\Delta_k} , \tag{52}$$

where γ_1 and γ_3 are the dipole decay constants for $a\leftrightarrow b$ and $b\leftrightarrow c$ transitions, $\Delta_1=\Delta_2-\Delta'$, and $\Delta_3=\Delta'$. Similarly, the matrix element ρ_{31} is found from the steady-state solutions of Eqs. (36) and (37)

$$\rho_{31}=\frac{-i\mathcal{D}_3[\mathcal{V}_3(f_c-\mathcal{D}_1^*\mathcal{D}_2^*|\mathcal{V}_2|^2)\rho_{1111}-\mathcal{V}_3 f_b\rho_{1010}+i\mathcal{V}_1^*\mathcal{V}_2(f_a\mathcal{D}_1^*-\mathcal{D}_2)\rho_{0011}]}{(1+\mathcal{D}_1^*\mathcal{D}_3|\mathcal{V}_2|^2)(1+I_2^2\mathcal{L}_2)} . \tag{53}$$

By substituting Eqs. (51) and (53) into Eq. (34) and using Eq. (32), we find the equation of motion

$$\begin{aligned}\langle n_1 n_3|\dot{\rho}|n_1 n_3\rangle=&-A_1(n_1+1)\langle n_1 n_3|\rho|n_1 n_3\rangle-A_1 n_1\langle n_1-1 n_3|\rho|n_1-1 n_3\rangle\\&-A_3(n_3+1)\langle n_1 n_3|\rho|n_1 n_3\rangle-A_3 n_3\langle n_1 n_3-1|\rho|n_1 n_3-1\rangle\\&+B_1(n_1+1)\langle n_1+1 n_3|\rho|n_1+1 n_3\rangle-B_1 n_1\langle n_1 n_3|\rho|n_1 n_3\rangle\\&+B_3(n_3+1)\langle n_1 n_3+1|\rho|n_1 n_3+1\rangle-B_3 n_3\langle n_1 n_3|\rho|n_1 n_3\rangle\\&-C_3\sqrt{n_1(n_3+1)}\langle n_1-1 n_3|\rho|n_1 n_3+1\rangle-C_3\sqrt{n_1 n_3}\langle n_1-1 n_3-1|\rho|n_1 n_3\rangle\\&-D_1\sqrt{(n_1+1)(n_3+1)}\langle n_1 n_3|\rho|n_1+1 n_3+1\rangle-D_1\sqrt{n_1(n_3+1)}\langle n_1-1 n_3|\rho|n_1 n_3+1\rangle ,\end{aligned} \tag{54}$$

where the coefficients A_1, B_1, A_3, B_3, C_3, and D_1 are given by

$$A_1=\frac{g_1^2\mathcal{D}_1}{1+I_2^2\mathcal{L}_2}\frac{f_a+I_2^2\mathcal{D}_3^*\mathcal{D}_2^*/4T_1T_2}{1+I_2^2\mathcal{D}_1\mathcal{D}_3^*/4T_1T_2} , \tag{55}$$

$$B_1=\frac{g_1^2\mathcal{D}_1}{1+I_2^2\mathcal{L}_2}\frac{f_b}{1+I_2^2\mathcal{D}_1\mathcal{D}_3^*/4T_1T_2} , \tag{56}$$

$$A_3=\frac{g_3^2\mathcal{D}_3}{1+I_2^2\mathcal{L}_2}\frac{f_b}{1+I_2^2\mathcal{D}_1^*\mathcal{D}_3/4T_1T_2} , \tag{57}$$

$$B_3=\frac{g_3^2\mathcal{D}_3}{1+I_2^2\mathcal{L}_2}\frac{f_c-I_2^2\mathcal{D}_1^*\mathcal{D}_2^*/4T_1T_2}{1+I_2^2\mathcal{D}_1^*\mathcal{D}_3/4T_1T_2} , \tag{58}$$

$$C_3=\frac{ig_3^2\mathcal{D}_3}{1+I_2^2\mathcal{L}_2}U_1^*U_3^*\mathcal{V}_2\frac{-f_a\mathcal{D}_1^*+\mathcal{D}_2}{1+I_2^2\mathcal{D}_1^*\mathcal{D}_3/4T_1T_2} , \tag{59}$$

$$D_1=\frac{ig_1^2\mathcal{D}_1}{1+I_2^2\mathcal{L}_2}U_1^*U_3^*\mathcal{V}_2\frac{f_c\mathcal{D}_3^*+\mathcal{D}_2}{1+I_2^2\mathcal{D}_1\mathcal{D}_3^*/4T_1T_2} . \tag{60}$$

We can write an operator equation that yields Eq. (60) by noting the properties of the creation and annihilation

operator for mode k

$$a_k^\dagger|n_k\rangle=\sqrt{n_k+1}\,|n_k+1\rangle$$

and

$$a_k|n_k\rangle=\sqrt{n_k}\,|n_k-1\rangle\ . \tag{61}$$

Using Equation (61) we finally find the equation of motion for ρ, the reduced density operator for the side-mode fields, in terms of the creation and annihilation operators of the side modes:

$$\begin{aligned}\dot{\rho}=&-A_1(\rho a_1 a_1^\dagger-a_1^\dagger\rho a_1)-(B_1+\nu/2Q)(a_1^\dagger a_1\rho-a_1\rho a_1^\dagger)\\&-A_3(\rho a_3 a_3^\dagger-a_3^\dagger\rho a_3)\\&-(B_3+\nu/2Q)(a_3^\dagger a_3\rho-a_3\rho a_3^\dagger)+C_3(a_3^\dagger a_1^\dagger\rho-a_1^\dagger\rho a_3^\dagger)\\&+D_1(\rho a_3^\dagger a_1^\dagger-a_1^\dagger\rho a_3^\dagger)+(\text{adjoint})\ .\end{aligned} \tag{62}$$

where ν/Q is the rate of cavity losses for mode 1 and 3.

The equations of motion for the number operator $a_k^\dagger a_k$ for mode k and combination tone operator a_1a_3 are easily obtained from Equation (62)

$$\frac{d}{dt}\langle a_1^\dagger a_1\rangle=\langle a_1^\dagger a_1\dot{\rho}\rangle=(A_1-B_1-\nu/2Q)\langle a_1^\dagger a_1\rangle-D_1^*\langle a_1a_3\rangle+A_1+\text{c.c.}\ , \tag{63}$$

$$\frac{d}{dt}\langle a_3^\dagger a_3\rangle=\langle a_3^\dagger a_3\dot{\rho}\rangle=(A_1-B_1-\nu/2Q)\langle a_3^\dagger a_3\rangle+C_3^*\langle a_1a_3\rangle+A_3+\text{c.c.}\ , \tag{64}$$

$$\begin{aligned}\frac{d}{dt}\langle a_1a_3\rangle&=\langle a_1a_3\dot{\rho}\rangle\\&=(A_1+A_3-B_1-B_3-\nu/Q)\langle a_1a_3\rangle\\&\quad-D_1\langle a_3^\dagger a_3\rangle+C_3\langle a_1^\dagger a_1\rangle+C_3\ .\end{aligned} \tag{65}$$

In free space, no build up of photon number occurs, and $d\langle n_k\rangle/dt=A_k+A_k^*$. Thus we interpret the inhomogeneous term $A_k+A_k^*$ of Eqs. (63) and (64) as the spectrum of resonance fluorescence for mode k. Figure 3 plots the centrally tuned spectrum of $A_1+A_1^*$ for $I_2=0.5$ and 20. For the strong-pump field of $I_2=20$, we note that the resonance fluorescence spectrum has only two peaks, both of which are at the Rabi frequencies, compared to the three peaks (two side peaks and one central peak) spectrum of the one-photon two-level case.[15] The difference A_k-B_k is the semiclassical complex gain coefficient for mode k. Similarly the inhomogeneous term C_3 of Eq. (65) is the source contribution for the quantum combination tone $\langle a_1a_3\rangle$, which is responsible for squeezing.[6,16] The real part of C_3 has two peaks at the Rabi frequencies for strong-pump fields as shown in Fig. 4, but unlike for A_1, one peak is negative.

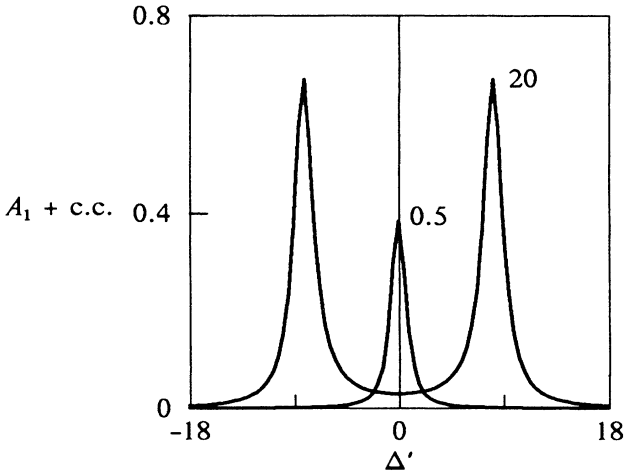

FIG. 3. Free-space resonance fluorescence spectrum A_1+c.c. vs Δ' for $I_2=0.5$ and 20, $\Delta_2=0$, $C=1$, $\Gamma_a=1$, $\Gamma_1=\Gamma_3=1$, and $\gamma_1=\gamma_3=\gamma_2=1$. All frequencies are in units of γ_2.

IV. APPLICATION TO SQUEEZING

The squeezed light results from a linear combination of the side-mode annihilation and creation operators a_1 and $a_3^\dagger$. A possible experimental configuration in a cavity is depicted in Refs. 1 and 6. The squeezed light may be measurable by means of a homodyne detection scheme[1] (note that for very large beat frequencies $\nu_2-\nu_1$, homodyne detection may be impractical). This homodyne detection permits the direct measurement of the variance for any relative phase shift θ of the local oscillator. The amplitude d of the squeezed field is

$$d=2^{-1/2}(a_1e^{i\theta}+a_3^\dagger e^{-i\theta})\ . \tag{66}$$

We define two Hermitian operators $d_{1,2}=(d\pm d^\dagger)/2$ and calculate the spectrum of their variances as discussed in

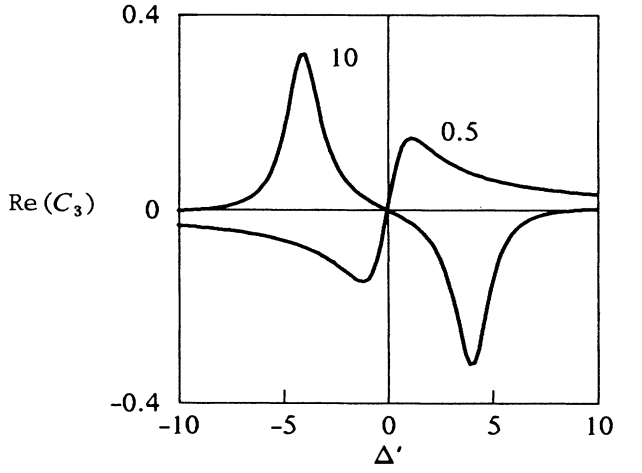

FIG. 4. Real part of C_3 for $I_2=0.5$ and 10. The other parameters are the same as in Fig. 3.

Ref. 6. The expression for the minimum variance outside the cavity is given by

$$\Delta d_1^2=\frac{1}{4}+\frac{1}{4}\frac{\nu}{Q}(\mathcal{S}_{12}+\mathcal{S}_{34}-2|\mathcal{S}_{13}|)\ , \tag{67}$$

where the spectral quantities $\mathcal{S}_{12}$, $\mathcal{S}_{13}$, and $\mathcal{S}_{34}$ are given by Eqs. (38)–(40) of Ref. 6 letting $C_1=D_3=0$ and using the coefficients given by Eqs. (55)–(60) of the present paper

$$\mathcal{S}_{12}=\frac{(\alpha_3-i\omega)(\alpha_3^*+i\omega)A_1+|D_1|^2A_3-(\alpha_3^*+i\omega)D_1^*C_3+\text{c.c.}}{|(\alpha_1+i\omega)(\alpha_3^*+i\omega)+D_1C_3^*|^2}\ , \tag{68}$$

$$\mathcal{S}_{13}=\frac{(\alpha_3^*+i\omega)C_3(A_1+A_1^*)-(\alpha_1^*-i\omega)D_1(A_3+A_3^*)+(\alpha_1^*-i\omega)(\alpha_3^*+i\omega)C_3-D_1|C_3|^2}{|(\alpha_1+i\omega)(\alpha_3^*+i\omega)+D_1C_3^*|^2}\ , \tag{69}$$

$$\mathcal{S}_{34}=\frac{(\alpha_1-i\omega)(\alpha_1^*+i\omega)A_3+|C_3|^2A_1+(\alpha_1^*+i\omega)C_3^*C_1+\text{c.c.}}{|(\alpha_3+i\omega)(\alpha_1^*+i\omega)+C_3D_1^*|^2}\ , \tag{70}$$

where the absorption coefficients $\alpha_k=B_k-A_k+\nu/2Q$.

Substituting Eqs. (68)–(70) into Eq. (67) and letting $\omega=0$, we calculate the squeezing variance Δd_1^2 as a function of the pump intensity I_2, the pump detuning Δ_2, the side-mode detuning Δ', and the cooperativity parameter[6] $C=Ng^2Q/\gamma_2\nu$, where we take $g_1=g_2=g$. Figure 5 shows the minimum variance Δd_1^2 given by Eq. (67) versus the side-mode detuning Δ' for $I_2=0.5$ and 150, $C=100$, and $\Delta_2=0$. We notice that for the low-intensity case there are two large regions with squeezing on either side of a small unsqueezed region around $\Delta'=0$. For pump intensities small enough to be treated by fourth-order perturbation theory, four-wave mixing is the dominant nonlinearity, since spontaneous-emission processes first show up in sixth-order perturbation theory. A lack of spontaneous emission aids in the generation of good squeezing. On the other hand, for strong-pump intensities, we obtain even better squeezing, namely, for Δ' values within the Rabi sidebands. This is due to the Rabi splitting of the upper level a accompanied by vanishing splitting of level b, which, as Fig. 3 shows, leads to negligible spontaneous emission for this tuning region.

Figure 6 plots the minimum variance versus the pump intensity in the center of this region ($\Delta'=0$) for various values of the cooperativity parameter C. We see that as C increases, squeezing is significantly enhanced for certain strong-pump intensities. In fact, we can get almost perfect squeezing by choosing suitable values of the cooperativity parameter and pump intensity (e.g., $\Delta d_1^2\cong 10^{-2}$ for $C=100$ and $I_2\cong 150$, and $\Delta d_1^2\cong 10^{-3}$ for $C=1000$ and $I_2\cong 1500$).

In conclusion, we have treated quantum multiwave interactions in a two-photon three-level cascade model. We have derived the explicit formula for the resonance fluorescence spectrum and have shown that the spectrum

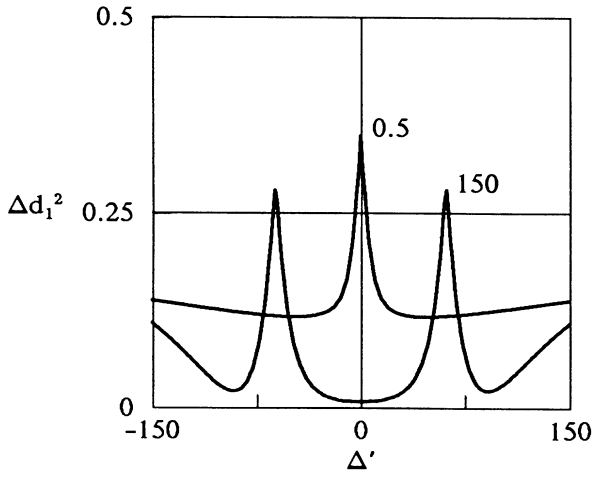

FIG. 5. Variance Δd_1^2 vs $\Delta'=(\omega_{bc}-\nu_2)-\Delta$ for $I_2=0.5$ and 150, $C=100$; the other parameters are the same as in Fig. 3.

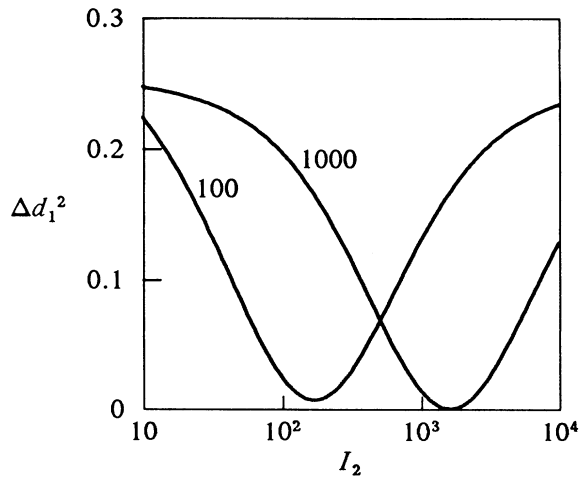

FIG. 6. Variance Δd_1^2 vs I_2 for $C=100$ and 1000, $\Delta'=0$; the other parameters are the same as in Fig. 3.

has only two peaks, compared to the three-peak spectrum of the one-photon two-level case. We have applied our theory to the generation of squeezed states of light and have shown that the two-photon three-level cascade model predicts broadband squeezing for low-pump intensities and excellent squeezing for strong-pump intensities in the vicinity of small side-mode detunings.

ACKNOWLEDGMENTS

This work was supported in part by the U. S. Office of Naval Research, in part by the U. S. Army Research Office, and in part by the U. S. Air Force Office of Scientific Research.

[1]R. E. Slusher, L. W. Hollberg, B. Yurke, J. C. Mertz, and J. F. Valley, Phys. Rev. Lett. **55**, 2409 (1985).

[2]R. M. Shelby, M. D. Levenson, S. H. Perlmutter, R. V. DeVoe, and D. F. Walls, Phys. Rev. Lett. **57**, 691 (1986).

[3]M. Maeda, P. Kumar, and J. H. Shapiro, Opt. Lett. **12**, 161 (1987).

[4]L. A. Wu, H. J. Kimble, J. L. Hall, and H. Wu, Phys. Rev. Lett. **57**, 2520 (1986).

[5]M. Sargent III, D. A. Holm, and M. S. Zubairy, Phys. Rev. A **31**, 3112 (1985).

[6]D. A. Holm and M. Sargent III, Phys. Rev. A **35**, 2150 (1987). Note, in Eq. (39), the term $+\chi_1\chi_3$ should be multiplied by $C_1^*+C_3^*$.

[7]M. Sargent III, S. Ovadia, and M. H. Lu, Phys. Rev. A **32**, 1596 (1985).

[8]D. A. Holm and M. Sargent III, Phys. Rev. A **33**, 1073 (1986).

[9]B. A. Capron, D. A. Holm, and M. Sargent III, Phys. Rev. A **35**, 3388 (1987).

[10]Sunghyuck An and M. Sargent III, Opt. Lett. **13**, 473 (1988).

[11]C. M. Savage and D. F. Walls, Phys. Rev. A **33**, 3282 (1986).

[12]M. S. Malcuit, D. J. Gauthier, and R. W. Boyd, Phys. Rev. Lett. **55**, 1086 (1985).

[13]R. W. Boyd, M. S. Malcuit, D. J. Gauthier, and K. Rzażewski, Phys. Rev. A **35**, 1648 (1987).

[14]G. S. Agarwal, Phys. Rev. Lett. **57**, 827 (1986).

[15]D. A. Holm, M. Sargent III, and S. Stenholm, J. Opt. Soc. Am. B **2**, 1456 (1985).

[16]D. A. Holm, M. Sargent III, and B. A. Capron, Opt. Lett. **11**, 443 (1986).